Journal of Ceramic Processing Research. Vol. 21, Special. 1, pp. s23~s27 (2020)
(Received 13 December 2019, Received in revised form 24 April 2020, Accepted 4 May 2020)
https://doi.org/10.36410/jcpr.2020.21.S1.s23

J O U R N A L O F
Ceramic Processing Research

Enhanced optical output power of AlGaN/GaN ultraviolet light-emitting diodes fabricated with breakdown induced conductive channels

Seonghoon Jeong[a], Sung-Nam Lee[b], Chel-Jong Choi[a,*] and Hyunsoo Kim[a,*]
[a]*School of Semiconductor and Chemical Engineering, Semiconductor Physics Research Center, Jeonbuk National University, Jeonju 54896, Korea*
[b]*Department of Nano-Optical Engineering, Korea Polytechnic University, Siheung 15073, Korea*

The enhanced optical output power of AlGaN/GaN deep ultraviolet light-emitting diodes (UV LEDs) were demonstrated by using the breakdown-induced conductive channels (BICCs). The BICCs could be made by electrical reverse biasing between two adjacent contact pads formed on top p-type layers with a certain distance, causing an electrical breakdown of pn junction and hence a generation of conductive channels. Accordingly, the reflective Ni/Ag/Pt electrodes could be formed simultaneously on the top p-type layer and the other p-type layer with the BICCs, acting as the p- and n-contacts, respectively. The deep UV LEDs fabricated with the BICCs produced the enhanced optical output power by 15 % as compared to the reference LEDs, which were fabricated with the conventional Ti/Al/Ti/Au layers formed on mesa-etched n-type layer. This could be due to the reduced light absorption at the n-contact pads, indicating that the use of BICCs will be very suitable for obtaining better output performance of deep UV emitters.

Keywords: Ultraviolet, Light emitting diodes, Breakdown-induced conductive channels, AlGaN/GaN.

Introduction

GaN-based light-emitting diodes (LEDs) are being widely used in a variety of applications such as displays, mobile communications, automotive lighting and interior/exterior lighting [1-3]. Recently, the deep ultraviolet light-emitting diodes (UV LEDs) fabricated with the AlGaN/GaN-based materials have drawn considerable attention owing to their potential applications with an extremely short emission wavelength of ~260 nm such as sterilization, medical treatment, purification, and bioindustry [4-7]. However, for faster commercialization, it is still necessary to improve the external quantum efficiency or to increase the optical output power of UV LEDs [1-7].

According to the literatures [8-14], the deep UV LEDs were found to suffer from very poor light extraction efficiency. This was due to the strong light absorption through the top p-GaN contact layer [8-10], the anisotropic optical polarization nature of AlGaN-based materials [8, 11, 12], and a significant total internal reflection occurring as a result of a large difference in the refractive indices between AlGaN-based semiconductors and substrate or air [8], [13-14]. Therefore, because the light experiences multiple internal reflections within a chip, it is quite crucial to suppress the absorption of trapped light by avoiding highly absorptive materials such as electrodes. The conventional metal electrodes used in the deep UV LEDs are Ag- and Ti/Al-based schemes as a reflective p-contact and a n-contact, respectively, because they are very suitable for the formation of Ohmic contact upon thermal annealing. However, the thermally annealed Ti/Al-based n-contacts are generally known to have lower optical reflectivity against the Ag.

Very recently, our group showed that the reverse breakdown mechanism of GaN-based LED, namely, the defect-assisted Zener breakdown. More specifically, the reverse biasing of GaN p-n junction wan shown to induce a local breakdown through the native crystal defects such as V-pits. Interestingly, this phenomenon resulted in a formation of conductive channels, which is so-called the breakdown-induced conductive channels (BICCs). By using BICCs, AC-controllable light-emitting devices without any AC–DC converter [15] or the flat-type InGaN-based LEDs without an n-contact electrode [16] could be demonstrated.

In this study, based on the BICCs method, we attempted to use the reflective Ni/Ag/Pt contact as the p- and n-electrodes for AlGaN/GaN deep UV LEDs simultaneously. By using the BICCs, the Ni/Ag/Pt contact could be served as the n-type electrodes as well as p-electrodes. The deep UV LEDs fabricated with the BICCs produced the enhanced optical output power by 15% as compared to the reference LEDs. This could be attributed to the reduced light absorption at the n-contact by 65%. These results indicate that the use of

*Corresponding author:
Tel : +82-63-270-3974
Fax: +82-63-270-3585
E-mail: cjchoi@jbnu.ac.kr (C.-J. Choi), hskim7@jbnu.ac.kr (H. Kim)

BICCs will be very suitable for obtaining better output performance of deep UV emitters as well as for reducing the process step of metal deposition.

Experimental

To fabricate the deep UV LEDs, commercially available AlGaN/GaN wafers (the peak emission wavelength of 273 nm) grown on c-plane sapphire substrate by metalorganic chemical vapor deposition were used. The structure of UV LEDs consisted of n-type AlGaN cladding layer, five periods of AlGaN/AlGaN multiple quantum wells, p-type AlGaN cladding layer, and a p-type GaN contact layer. Fig. 1(a) shows the schematic fabrication procedure of reference UV LEDs. For device fabrication, the mesa was defined by conventional photolithography and dry etching by inductively coupled plasma reactive ion etching system. The etching depth was about 400 nm. As the n-electrode, the 20/60/20/100 nm-thick Ti/Al/Ti/Au layers were then e-beam evaporated on the exposed n-AlGaN layer, followed by rapid thermal annealing (RTA) at 950 ºC for 1min in N_2. As the p-electrodes, 2/200/30 nm-thick Ni/Ag/Pt layers were deposited on p-AlGaN, followed by RTA at 550 ºC for 1 min in air. In addition, the schematic fabrication procedure of UV LEDs having BICCs (referred hereto as 'BICCs-LEDs') is shown in Fig. 1(b). First, the mesa was also defined by dry etching, while it should be noted that the small circular mesa was additionally defined at the expected position of n-electrodes. Then, the Ni/Ag/Pt layers were deposited on the top of each mesa simultaneously, followed by RTA at 550 ºC for 1 min in air. To generate the BICCs, the alternating electrical biasing (± 15 V with a compliance current of 40 mA) was performed between two adjacent contact pads, in which the electrical junction breakdown occurs. To investigate the contact properties, transmission line model (TLM) patterns were also formed on the same wafer [17], in which the same method to generate BICCs was carried out. The electrical and optical characteristics of the fabricated devices were measured using a probestation system with parameter analyzer (HP4156A), photodiode (883-UV), and optical spectrometer (Ocean Optics USB2000).

Results and Discussion

Fig. 2(a) shows the current-voltage (*I-V*) curves of Ni/Ag/Pt contact formed on the top p-GaN layer as a function of reverse biasing. For this study, the TLM patterns having the pattern size of 200 × 100 mm^2 and a pad spacing of 5 μm was used (see the inset of Fig. 2(a)). Note that the junction breakdown occurs at reverse voltage lower than -15 V with the first *I-V* sweep. The additional *I-V* sweeps produced an insignificant change of *I-V* curve, i.e., the generation of BICCs originating from the junction breakdown through the V-defects were nearly saturated [15, 18, 19]. As shown in the inset of Fig. 2(a), a number of black spots were observed after electrical reverse biasing. The measurements of SEM and EDX mapping on this black spot showed that, first, the metal electrode is exploded and, second, the BICCs were formed through the epitaxial V-defects [15] (Fig. 2(b)). The explosion and hence the peeling-off phenomenon of metal electrode seems to be due to the extremely large electrical resistivity of AlGaN epitaxial films [20].

Fig. 3(a) shows *I-V* characteristics of the Ni/Ag/Pt contact formed on BICCs as a function of the pad spacing. The *I-V* curves showed a pad-spacing dependence, indicating that the TLM method is valid [17]. However, the current level of contact was quite low, resulted in the very high specific contact resistance (ρ_{sc}) of 0.61 Ωcm^2. This indicates that, although the BICCs resulted in a current flow across junction from the top p-layer to bottom n-layer (see the inset of Fig. 2(b)), the amount of current flow is insufficient, i.e., the density of electrical conduction path is limited. Indeed, this is

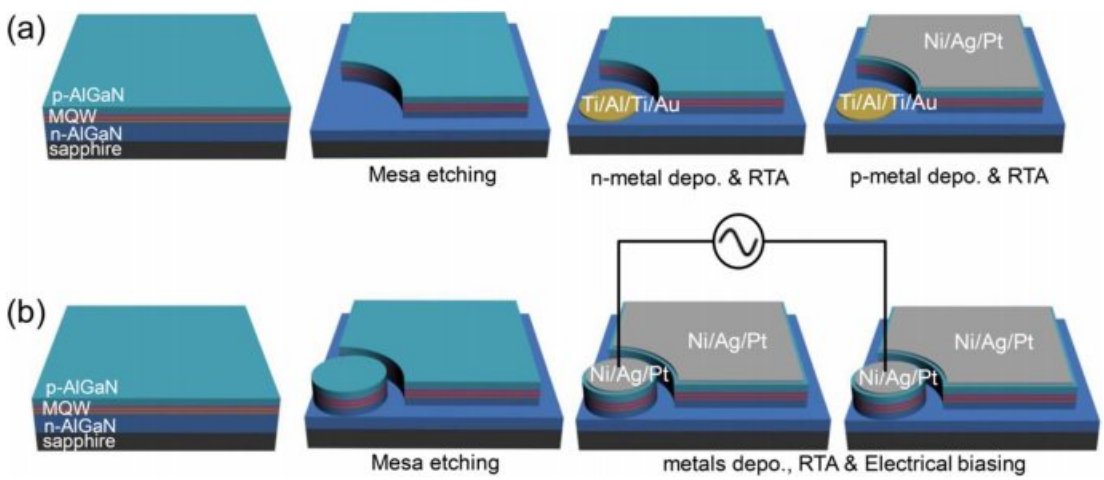

Fig. 1. Schematic fabrication procedures for (a) reference LEDs and (b) BICCs-LEDs.

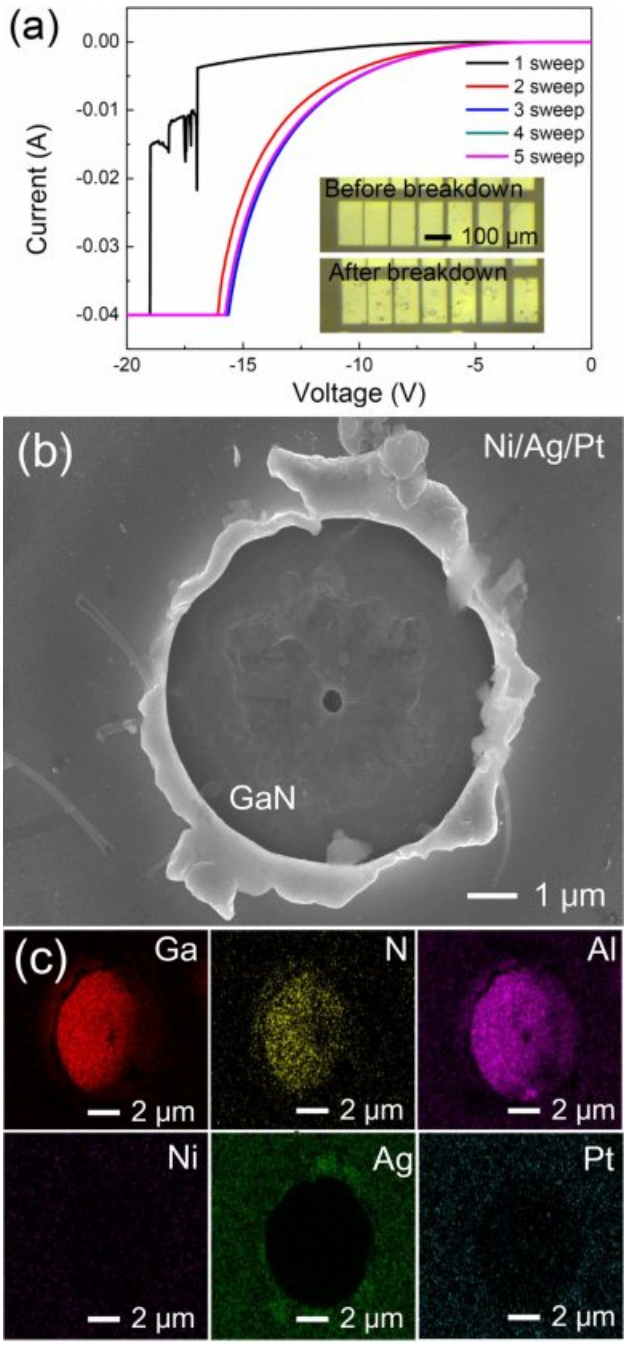

Fig. 2. (a) *I-V* curves of Ni/Ag/Pt contact formed on the top p-GaN layer as a function of reverse biasing. The inset shows the optical microscopic image of the TLM patterns before and after breakdown. (b) SEM image and (c) EDX mapping images of TLM patterns after breakdown by reverse biasing.

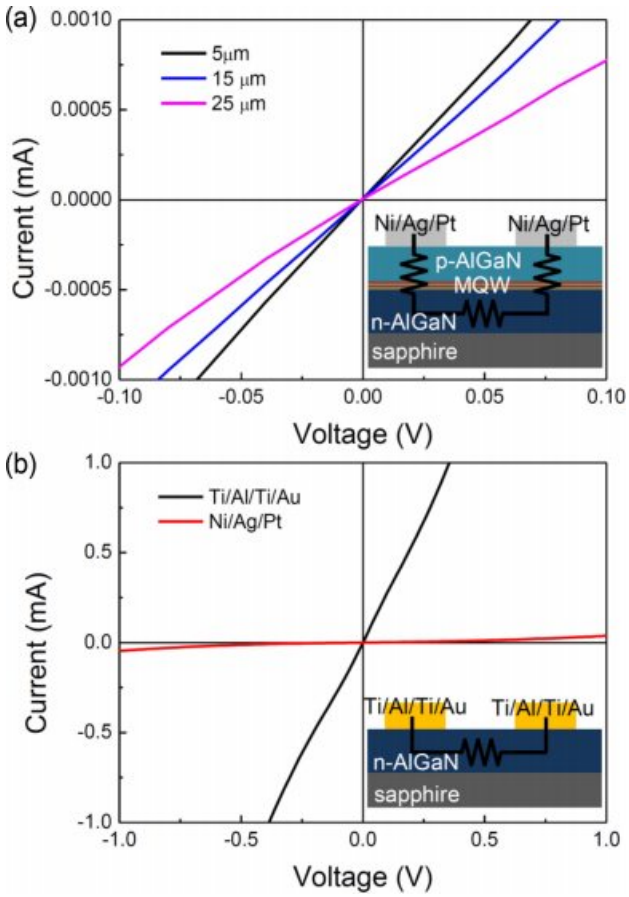

Fig. 3. (a) *I-V* characteristics of the Ni/Ag/Pt contact formed on BICCs-generated conduction layer as a function of the pad spacing. The inset shows the schematic cross-sectional diagram of current flow across BICCs. (b) *I-V* curves of Ni/Ag/Pt formed on BICCs and the conventional Ti/Al/Ti/Au formed on n-AlGaN layer. The inset shows the schematic current flow of conventional n-contact.

different from our previous findings that the generation of BICCs led to a significant current flow across the junction in the InGaN/GaN-based blue LEDs [15]. As shown in Fig. 2(b), this is presumably due to the peeling-off of metal electrode after BICCs formation, i.e., the although the BICCs is generated, the conduction through BICCs would be very limited due to the absence of metal contacts.

Fig. 3(b) shows the *I-V* curves of Ni/Ag/Pt formed on BICCs and the conventional Ti/Al/Ti/Au formed on n-AlGaN layer (mesa etched surface), where the pad spacing was 5 mm. The current flow of conventional Ti/Al/Ti/Au contact is schematically drawn as shown in the inset of Fig. 3(b). It is clear that the Ti/Al/Ti/Au formed on n-AlGaN layer has much steeper *I-V* curve than the Ni/Ag/Pt formed on BICCs. Accordingly, the specific contact resistance of Ti/Al/Ti/Au on n-AlGaN was measured to be 8.48×10^{-3} Ωcm^2. This result indicates that the contact properties of Ni/Ag/Pt on BICCs still need to be further improved by optimizing the density of BICCs.

Fig. 4(a) shows the *I-V* curves of the reference LEDs and the BICCs-LEDs. Consistently, the reference LEDs showed superior *I-V* curves against the BICCs-LEDs. For example, the forward voltages measured at injection current of 20 mA were 9.4 V and 14.6 V for the reference LEDs and BICCs-LEDs, respectively. This is essentially due to the worse contact properties of Ni/Ag/Pt on BICCs over the Ti/Al/Ti/Au on n-AlGaN.

Nevertheless, the optical output properties of the

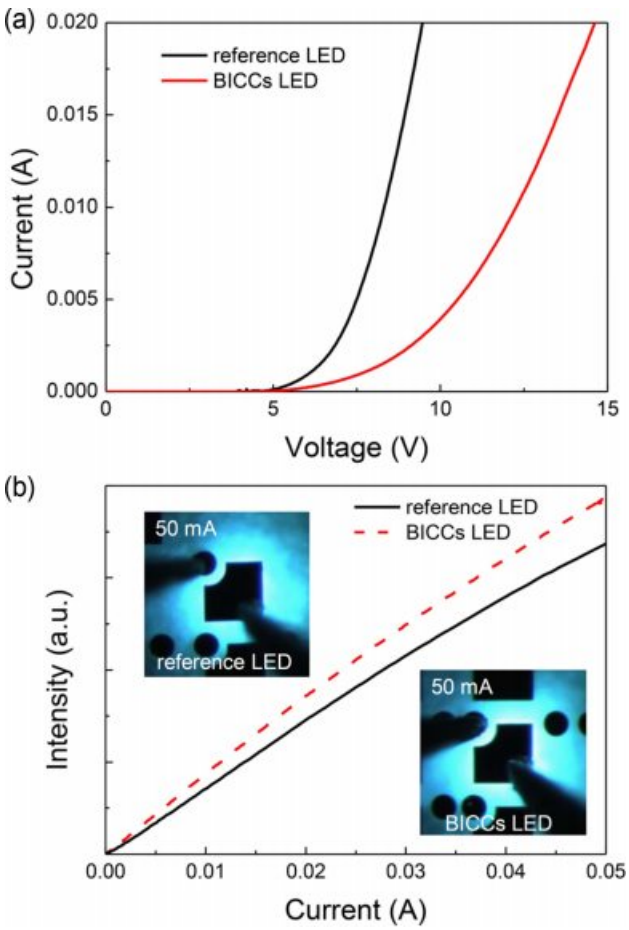

Fig. 4. (a) Typical *I-V* curves of reference LEDs and BICCs-LEDs. (b) The optical output power verse current curve of reference LEDs and BICCs-LEDs. The inset show the EL image of both LEDs taken at injection current of 50 mA.

BICCs-LEDs were significantly improved as compared to the reference LED (Fig. 4(b)). For example, the optical output power of BICCs-LEDs was about 15% higher than that of the reference LEDs when measured at injection current 50 mA. Here, the optical output power was measured using the photodiodes, which were placed bottom side of LED wafers. A noticeable output enhancement is attributed to the higher optical reflectivity of thermally annealed Ni/Ag/Pt contact than that of annealed Ti/Al/Ti/Au.

Indeed, it is generally known that the optical reflectivity of Ag is highest among metals in the visible wavelength range (> 400 nm) [21]. However, the optical reflectivity of Ag drops significantly at the wavelength below 400 nm. On the one hand, the Al metal is known to show the highest optical reflectivity at the deep UV wavelength range (< 300 nm), while the Ti has poor reflectivity. However, it should be noted that the metal electrodes are thermally annealed for the formation of Ohmic contact. During the annealing process, each metal can interdiffuse depending on their thermodynamic tendency. In other words, this indicates that the optical reflectivity

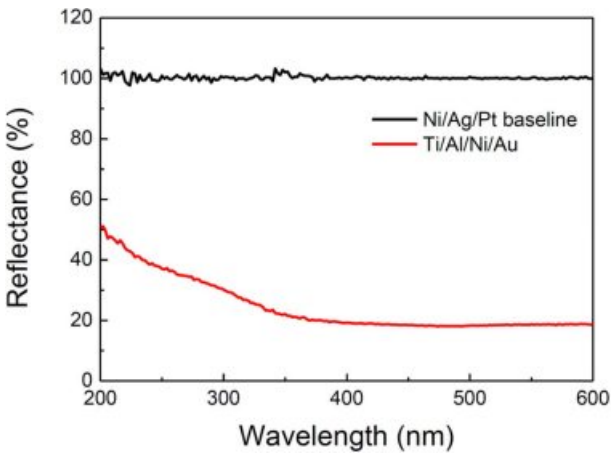

Fig. 5. The relative optical reflectance spectra of thermally annealed Ni/Ag/Pt and Ti/Al/Ti/Au electrodes.

of electrodes should be compared after thermal annealing. Fig. 5 shows the relative optical reflectance spectra of thermally annealed Ni/Ag/Pt and Ti/Al/Ti/Au prepared on both-side polished sapphire substrates. For this measurements, the optical reflectance spectra of annealed Ni/Ag/Pt were set as the base line of 100%. Note that, at the wavelength of 273 nm, the optical reflectance of annealed Ni/Ag/Pt was ~65% higher than that of annealed Ti/Al/Ti/Au. Therefore, the enhanced optical output power of BICCs-LEDs is explained.

Conclusions

In summary, the optical output power of AlGaN/GaN deep UV LEDs could be improved by using reflective Ni/Ag/Pt contact and BICCs. By using BICCs, the Ni/Ag/Pt contacts could be used as the p- and n-type electrodes simultaneously. Besides the simpler and cost-comparative process step, the Ni/Ag/Pt contact showed much higher optical reflectivity than the reference Ti/Al/Ti/Au contact. Accordingly, the UV LEDs fabricated with the Ni/Ag/Pt and BICCs produced 15% higher optical output power than the reference LEDs. This indicates that, if the electrical contact properties are further improved, the BICCs method combined with the use of reflective metal contact would be promising for improving the output efficiency of deep UV LEDs.

Acknowledgments

This work was supported by Samsung Research Funding Center of Samsung Electronics under Project Number SRFC-IT1501-06, and by the Technology Innovation Program (Leading design of future environment products using advanced photocatalytic purification sterilization technology) (Project No. 20006767) funded by the Ministry of Trade, Industry & Energy, Republic of Korea.

Reference

1. M. R. Krames, O. B. Shchekin, R. Mueller-Mach, G. O.Mueller, L. Zhou, G. Harbers, and M. G. Craford, J. Disp. Technol. 3 (2007) 160-175.
2. S. Nakamura, T. Mukai, and M. Senoh, Jpn. J. Appl. Phys. 30 (1991) L1708-L1711.
3. J. J. Wierer, D. A. Steigerwald, M. R. Krames, J. J. O'Shea, M. J. Ludowise, G. Christenson, Y. C. Shen, C. Lowery, P. S. Martin, S. Subramanya, W. G. W. Götz, N. F. Gardner, R. S. Kern, and S. A. Stockman, Appl. Phys. Lett. 78[22] (2001) 3379-3381.
4. H. Kudo, M. Sawai, Y. Suzuki, X. Wang, T. Gessei, D. Takahasho, T. Arakawa, and K. Mitsubayashi, Sens. Actuator B-chem. 147 (2010) 676-680.
5. J. Close, J. Ip, K. H. Lam, Renew. Energy 31 (2006) 1657-1664.
6. J. L. Shie, C. H. Lee, C. S. Chiou, C. T. Chang, C. C. Chang, C. Y. Chang, J. Hazard. Mater. 155 (2008) 164-172.
7. M. Kneissl, T. Seong, J. Han, and H. Amano, Nat. Photonics 13 (2019) 233-244.
8. Y. Cuo, J. Yan, Y. Zhang, J. Wang, and J. Li, J. Nano-photonics 12[4] (2018) 043510.
9. H. Ryu, I. Choi, H. Choi, and J. Shim, Appl. Phys. Express 6 (2013) 062101.
10. M. Akiba, H. Hirayama, Y. Tomita, Y. Tsukada, N. Maeda, and N. Kamata, Phys. Status Solidi C. 9[3/4] (2012) 806-809.
11. P. Dong, J. Yan, Y. Zhang, J. Wang, C. Geng, H. Zheng, X. Wei, Q. Yan, and J. Opt. Express 22[S2] (2014) A320-A327.
12. S. Zhao, M. Djavid, and Z. Mi, Nano Lett. 15[10] (2015) 7006-7009.
13. N. Maeda and H. Hirayama, Phys. Status Solidi C 10[11] (2013) 1521-1524.
14. M. Shatalov, W. Sun, A. Lunev, X. Hu, A. Dobrinsky, Y. Bilenko, J. Yang, M. Shur, R. Gaska, and C. Moe, Appl. Phys. Express 5[8] (2012) 082101.
15. S. Han, S. Baek, H. Lee, H. Kim, and S. Lee, Sci. Rep. 8 (2018) 16547.
16. S. Baek, H. Lee, and S. Lee, Sci. Rep. 9 (2019) 13654.
17. G. K. Reeves and H. B. Harrison, IEEE Electron. Device Lett. 3(1982) 111-113.
18. X. H. Wu, C. R. Elsass, A. Abare, M. Mack, S. Keller, P. M. Petroff, S. P. DenBaars, and J. S. Speck, Appl. Phys. Lett. 72 (1998) 692-694.
19. H. K. Cho and J. Y. Lee, Appl. Phys. Lett. 79 (2001) 215-217.
20. S. Jeong, M. S. Kim, S. Lee, and H. Kim, Mat. Sci. Semicon. Proc. 90 (2019) 72.
21. H. Kim, K. H. Baik, J. Cho, J. W. Lee, S. Yoon, H. Kim, S. Lee, C. Sone, Y. Park, and T. Seong, IEEE Photonics Technol. Lett. 19 (2007) 336-338.